

JAERI-Tech
2001-082



JP0250012



DEVELOPMENT OF MAGNETIC $j \times B$ SENSOR

December 2001

Satoshi KASAI, Takahide NAKAYAMA* and Etsuo ISHITSUKA

日本原子力研究所
Japan Atomic Energy Research Institute

本レポートは、日本原子力研究所が不定期に公刊している研究報告書です。
入手の問合わせは、日本原子力研究所研究情報部研究情報課（〒319-1195 茨城県那珂郡東海村）あて、お申し越してください。なお、このほかに財団法人原子力弘済会資料センター（〒319-1195 茨城県那珂郡東海村日本原子力研究所内）で複写による実費頒布をおこなっております。

This report is issued irregularly.

Inquiries about availability of the reports should be addressed to Research Information Division, Department of Intellectual Resources, Japan Atomic Energy Research Institute, Tokai-mura, Naka-gun, Ibaraki-ken 319-1195, Japan.

© Japan Atomic Energy Research Institute, 2001

編集兼発行 日本原子力研究所

Development of Magnetic $j \times B$ Sensor

Satoshi KASAI, Takahide NAKAYAMA*

and Etsuo ISHITSUKA⁺

Department of Fusion Engineering Research

Naka Fusion Research Establishment

Japan Atomic Energy Research Institute

Naka-machi, Naka-gun, Ibaraki-ken

(Received November 5, 2001)

The improved mechanical sensor, i.e. magnetic $j \times B$ sensor (a mechanical sensor and a part of the steady state hybrid-type magnetic sensor) has been designed. The basic structure of the sensor is similar to the previously developed sensor (old sensor) in EDA phase. In this design, the neutron resistant materials are selected for the load cell (strain gauge and sensor beam) and sensing coil/ frame. In order to reduce temperature drift of the sensor signal, four strain gauges with the same electrical property and geometrical size are bonded on the sensor beam by using Al_2O_3 plasma spraying process, i.e., a couple of strain gauges is bonded on one side of the beam and another couple of gauges is bonded on the other side. These four strain gauges form an electrical bridge circuit.

The zero-level drift of the output of the load cell used in the magnetic $j \times B$ sensor was reduced to about 1/20 compared with the old sensor. The temperature dependence of the output of the load cell is small. The linearity of the output of the load cell against weight was obtained. A non-linearity was observed in the sensitivity of the magnetic $j \times B$ sensor. The deviation of sensitivity from the fitting line was less

This R&D was carried out under the ITER EDA task agreement of R&D task (Task agreement number : N 55 TT 08 FJ, Task number : T496).

⁺ Department of JMTR Oarai Research Establishment

* Hitachi, Ltd.

than 7 % in the high magnetic field region. The neutron irradiation effect on sensitivity of the sensor was investigated.

The sensitivity of the sensor was gradually decreased by ~ 30 % at neutron fluence of $(1.8 \sim 2.8) \times 10^{23} \text{ n/m}^2$ in the high magnetic field. During irradiation, the non-linearity was observed in the sensitivity.

Keywords : Magnetic $\mathbf{j} \times \mathbf{B}$ Sensor, Steady State Magnetic Sensor, Hybrid Magnetic Sensor, Diagnostics, ITER, Irradiation Test

jxB磁場計測センサーの開発

日本原子力研究所那珂研究所核融合工学部

河西 敏・中山 尚英*・石塚 悦男⁺

(2001年11月5日受理)

改良型のjxB磁場計測センサー（機械式センサーであり、ハイブリッド式定常磁場計測センサーの一部）を設計、製作した。そのセンサーの基本構造は、以前開発したセンサーと同じであるが、センサーに使用したロードセル（歪ゲージとセンサービームから構成されている）とセンシングコイルの材質には、中性子照射に耐えるものを採用した。センサー出力の温度によるドリフトを少なくするため、電気的特性、幾何学的大きさが同じ歪ゲージ2枚を一組として、センサービーム(SUS316L製)の表と裏にアルミナ(Al_2O_3)溶射により張り付けて、ロードセルを製作した。この4枚の歪ゲージがホイートストンブリッジを構成するように接続して、温度による出力のドリフト低減をはかった。

荷重、加熱、磁場試験及び中性子照射試験の結果、以下のことが分かった。jxB磁場計測センサーに使用するロードセル出力の零ドリフトを、以前開発したものに比べ、約1/20に減らすことができた。ロードセル出力の温度依存性は小さかったが、荷重に対するロードセル出力及びセンサー感度は非直線性を示した。jxB磁場計測センサー感度の最小二乗フィッティングラインからのずれは、高磁場で7%以下であった。このセンサーの感度が中性子照射で受ける影響について調べた。中性子照射量が $1.8\sim 2.8\times 10^{23} \text{ n/m}^2$ のとき、感度は高磁場では約30%減少することが分かった。照射中も感度に非直線性が観測された。

本開発は、ITER工学R&Dの一環として行ったものであり、R&Dタスク (Task agreement number : N 55 TT 08 FJ、Task ID number:T496) に基づくものである。

那珂研究所：〒311-0193 茨城県那珂郡那珂町向山801-1

+ 大洗研究所材料試験炉部

* (株) 日立

This is a blank page.

Contents

1. Introduction -----	1
2. Technical Outline -----	1
2.1 Items of R&D -----	1
2.2 Items of Test -----	2
3. Design and Fabrication of an Improved Magnetic $j \times B$ Sensor -----	2
4. Pre-irradiation Tests -----	4
5. Irradiation Tests -----	6
6. Summary -----	7
Acknowledgements -----	8
References -----	8

目 次

1.はじめに-----	1
2.技術概要-----	1
2.1 R&D項目-----	1
2.2 試験項目-----	2
3.改良型 $j \times B$ 磁場計測センサーの設計、製作-----	2
4.照射前の特性試験-----	4
5.照射試験-----	6
6.まとめ-----	7
謝辞-----	8
参考文献-----	8

This is a blank page.

1. Introduction

Measurement of the magnetic field under quasi-steady state conditions is important for long pulse operations in the International Thermonuclear Experimental Reactor (ITER)[1~6]. Present inductive methods using a conventional magnetic probe have a limit of time integration in the range over several thousand seconds. A new concept of a hybrid magnetic sensor is a combination of a conventional magnetic probe and a magnetic $j \times B$ (mechanical sensor). The former measures the magnetic field with low frequency and the latter measures the field with high frequency. The details of the principle and the mechanism are described in Refs.[1],[2] and [5]. To demonstrate feasibility of the hybrid magnetic sensor, the evaluation of the drifts and the responses and the long time measurement tests were carried out using the JT-60U tokamak discharges[1,2].

In the Engineering Design Activity (EDA) phase of ITER, this magnetic $j \times B$ sensor has been designed and manufactured to investigate the linearity of sensitivity, drift of the output signal of the sensor, effect of sensitivity under the baking and gamma-ray irradiation conditions[5,6].

The objectives of the R&D in EDA extension phase are to design and fabricate an improved mechanical sensor of the hybrid type magnetic $j \times B$ sensor, and also to examine the sensitivity to the baking temperature and the magnetic field in the absence of the neutron irradiation. Another objective is to investigate the sensitivity to the magnetic field by the in-situ measurement under the neutron irradiation. Irradiation was carried out to the fluence of $3.6 \times 10^{23} \text{ n/m}^2$ in the fission reactor, JMTR, at JAERI Oarai under the R&D task T492.

2. Technical Outline

2.1. Items of R&D

- (1) Design of an improved model of mechanical sensor for the magnetic $j \times B$ sensor
- (2) Fabrication of the magnetic $j \times B$ sensor
- (3) Sensitivity study of the magnetic $j \times B$ sensor

2.2. Items of Test

(1) Pre-irradiation sensitivity test

Temperature : RT ~ 200 °C

Magnetic field by external coil (solenoid coil) : 0 ~ 50 Gauss

(2) Irradiation test in JMTR under Task T492

Fluence : $\sim 1 \times 10^{24}$ n/m²

Temperature : ~ 200 °C

3. Design and Fabrication of an Improved Magnetic $j \times B$ Sensor

In previous work during the EDA phase, the prototype magnetic $j \times B$ sensor (mechanical sensor), which consists of the sensing coil/frame, sensing coil support, a load cell and a sensor beam, was designed, manufactured, and tested before the irradiation and under the neutron irradiation. This sensing coil was made of the copper wire coated with polyimide insulator and the wire was wound by 60 turns on a sensing coil frame made of aluminum. The sensing coil was supported by thin phosphor bronze plates on the both sides of the load cell. Also, the sensing coil/frame was connected with the load cell by the sensor beam (beryllium copper). The material of the joint between the frame and the beam was a thin phosphor plate. A strain gauge of constantan was the load cell. A pair of such strain gauges was pasted on the beam by phenol bonding. This work showed the basic viability of this type of sensor. The initial radiation test showed good performance after substantial gamma dose (about 7.2×10^6 Gy). However, temperature drift of the sensor signal was observed, causing a degradation of the measurement accuracy. Also, it was found necessary to improve the radiation resistance of the sensor.

In the present task T496 during the EDA-extension phase, further work was undertaken to reduce the effects of the operation temperature on the sensitivity, to reduce the size of the sensor, and to improve the resistance to neutron radiation. The basic structure of the magnetic $j \times B$ sensor (mechanical sensor) is similar to the prototype sensor developed in EDA phase. It is important to select materials with a low nuclear heating rate to suppress excessive heating by neutron irradiation in the fission reactor, JMTR.

Figure 1 shows the top view and the side view of the newly designed magnetic $j \times B$ sensor. The sensor consists of a load cell, sensing coil/frame, sensing

coil support, joint mechanism, mechanical sensor support and lead wires. The material of the strain gauge is a nickel-chromium (Kyowa Co. Ltd. : KG-873-NiCr). The size of a resistance pattern of the strain gauge is 3.5×5 mm. The resistance patterns are made of the same rod. This is very important to reduce the zero-level drift of the signal by changing temperature. Four active gauges are located on the stainless steel (SS 316) sensor beam. A couple of strain gauges is bonded on one side of the beam by ceramic (Al_2O_3) plasma spray coating, and another couple of strain gauges is bonded on the other side, forming an electrical bridge circuit as shown in Fig. 2. The voltage applied to the bridge is 5 volts in all measurements. The current that can be supplied to strain gauges limits this voltage. Usually, 2 volts is optimum for the present gauges, but in order to obtain large output of the sensor, 5 volts is applied to the bridge in present tests. With this arrangement, the zero-level drift of the sensor signal due to the change of temperature is automatically compensated if the four active gauges have the same electrical property and geometrical size and also the four gauges are bonded on both sides of the sensor beam geometrically symmetrically. So, the temperature drift of the output signal observed in the previous sensor is expected to be reduced. The thickness of the ceramic (Al_2O_3) plasma spray coating is about 250 μm and the sensor beam is 0.5 mm thickness. The sensor beam is mounted on the mechanical sensor support (Al 5052), which is mounted on the inner wall of the capsule in JMTR and is a heat sink. Mineral insulated cable (MI-cable : sheath material is SS316L, core is copper, insulator is MgO) with 0.5 mm in diameter is used as a lead wire of the signal. The bulk of the sensor-beam is made of stainless steel (SS316L) and the part of the beam connected with the sensing coil is made of aluminum (Al 5052) to conduct the excessive heat of the sensing coil generated by nuclear heating during irradiation in JMTR to heat sink (mechanical sensor support) through the sensor beam well.

A frame of the sensing coil is aluminum (Al 5052). The coil is made of the MI-cable with 0.5 mm in outer diameter (inner conductor : Cu, 0.2 mm ϕ) and the number of turns is more than 100. The sensing coil/frame is supported by the pivot mechanism, which is mounted on the mechanical sensor support. This mechanism is better than the old one that used a thin phosphor bronze plate because the property of Young's modulus might be degraded by neutron irradiation in the neutron environment. A flexible link between the sensing coil/frame and the sensor beam (load cell), which is the same mechanism of the old sensor, is adopted to eliminate

the noise caused by the thermal expansion stress of the sensing coil frame. The material of this link is inconel.

The main size of the sensor is 126 mm in length and 42 mm in width, respectively. The size is reduced by $\sim 20\%$ in length and $\sim 40\%$ in width compared with the size of the previous sensor. It may be possible to reduce the size of the magnetic $j \times B$ sensor up to the size of 20 mm in width and 100 mm in length that is required in the present design of the ITER-FEAT.

The temperature near the strain gauges is monitored by a thermocouple (K-type, 1.0 mm in diameter) as shown in Fig. 1.

In tests of linearity and sensitivity of the sensor in the magnetic field during the neutron irradiation, two solenoid coils were used to generate the magnetic field on the sensing coil, arranged on the top and the bottom of the magnetic $j \times B$ sensor and mounted on the inner wall of the capsule of JMTR as shown in Fig 1. These coils are made of MI-cable with 0.5 mm in diameter. About 1000 turns are wound on the aluminum coil frames (bobbins). The coils can generate about 250 Gauss at maximum on the sensing coil. These coils were used both in pre-irradiation test and in irradiation test.

The temperature near the strain gauges during the neutron irradiation was estimated by using the 3 dimensional simulation ABAQUS code. In this calculation, the gamma-heating rate is assumed to be 2.3 W/g (maximum heating rate at the assigned position of the capsule in JMTR). Aluminum heat sinks are located in the gaps between sensing coil, sensor beam, solenoid coils and capsule to conduct excessive heat by nuclear heating to capsule as shown in Fig. 1. The capsule is cooled by water. Estimated temperatures of the strain gauge, sensor beam (stainless steel SS316L) and sensing coil are 171 °C, 140~600 °C and 450~500 °C, respectively. The temperature increase of the sensor and the removal of the heat from the sensor must be considered in practice for the ITER-FEAT design. Figure 3 is a photograph during assembling of the magnetic $j \times B$ sensor.

4. Pre-Irradiation Tests

The zero level drift of the output of the load cell was checked. Figure 4 shows the dependence of the zero-level drift on the temperature, which was taken without weight on the load cell. Signals of the load cell were monitored by a commercially

available strain gauge amplifier including a display, power supply of the bridge circuit etc. (WGA-710A-4 : Kyowa Electric Instruments Ltd.). The zero level was gradually shifted with the temperature increase, but it is about 1/20 smaller than that of the old magnetic $j \times B$ sensor. This result indicates that the zero level drift is improved by using the active strain gauge bridge arrangement (Fig. 1) compared with the old sensor.

A linearity of the load cell was investigated in the temperature range of the room temperature (RT) to 240 °C in a loading test using standard copper weights. Figure 5 indicates the dependence of the output of the load cell on temperature. In this figure, the zero-level drift was subtracted from the output of the load cell. A gradual increase of the output was observed except in the data for 4.6 g, although some data were scattered. The increase of the output with temperature is small, i.e. temperature dependence of the load cell is weak. The resistance of 4 strain gauges increases with temperature rise according to the change of the specific resistivity with temperature. Unbalance among 4 resistances of strain gauges is small, i.e. less than 1 %. Figure 6 shows the output of the load cell against weight in different temperatures. A slight non-linearity was observed. Fitting lines are obtained by using the fitting method of least squares. A deviation of the output from the fitting line is less than 8 % at each temperature.

Magnetic field tests of the magnetic $j \times B$ sensor were carried out by assembling the sensor and solenoid coils in the dummy frame as shown in Fig. 7. Also, the assembled sensor and coils were installed in the electric oven (maximum heating temperature = 250 °C) for heating test. An external magnetic field was applied by two solenoid coils. A standard gauss meter was used to calibrate the magnetic field generated by solenoid coils and a calibration curve of magnetic field was obtained against the current of solenoid coils. In the test, the solenoid coils was excited first and after that the sensing coil was excited for short time (a few second). This process (ramp-up and ramp-down of the current of the coils) was repeated at each magnetic field. Two constant-current power supplies were used to keep the currents of solenoid coils and the sensing coil. The externally applied magnetic field was changed from 0 to 250 Gauss. The current of the sensing coil is fixed to 1A in all tests. This current was chosen so that the maximum movement of the edge of the sensing coil frame by tilting is about 0.2mm, i.e. $\sim 1/5$ of 1mm gap between the edge of the sensing coil frame and heat sink in Fig.1 in the external magnetic field of 250 Gauss.

Polarity of the current of the sensing coil was not changed in tests. If polarity is changed, the direction of tilting of the sensing coil is changed and the performance of the magnetic $j \times B$ sensor may be changed. When the direction of the poloidal magnetic field of ITER-FEAT is changed in the actual measurement of field, it may be better to keep the tilting-direction of the sensing coil unchanged by reversing the polarity of the sensing coil current for the above-mentioned reason.

The sensitivity of the sensor against the magnetic field was studied. The sensitivity is defined by the ratio of the output of the sensor to the voltage applied the bridge. The voltage applied to the bridge is 5 volts. Figure 8 shows the sensitivity of the sensor obtained in the heating test at temperature of 150, 200, 240 °C. The sensitivity was obtained by using the output of the sensor subtracted the zero-level drift. In this figure, the sensitivity is proportional to the magnetic field, but a slight non-linearity was observed. A maximum deviation of the sensitivity from the fitting line is within 7 % in the range of 0 ~ 250 Gauss using several measurements for the same temperature, with a different magnetic field. The reproducibility of the measurement for the same temperature and one magnetic field is high, namely within 3 %.

In future, it is necessary to make more improvement of the sensor concerning the measurement accuracy, reproducibility and linearity against weight and magnetic field.

5. Irradiation Tests

The magnetic $j \times B$ sensor and two solenoid coils are installed in the capsule for irradiation test as shown in Fig.1. The fast neutron (> 1 MeV) flux near the position of the sensor in the capsule is about 1.7×10^{17} n/m²/s (full power of JMTR is 50 MW and its flux is 2.1×10^{17} n/m²/s). The sensitivity and linearity of the sensor were obtained in three different phases, namely before operation, the power-up phase and the full-power phase. In these tests, the sensing coil and the solenoid coils were excited in the same way as pre-irradiation, and the sensing coil current is 1 A. The polarity of the current of the sensing coil was not changed.

Figure 9 shows the sensitivity of the sensor versus the external magnetic field in different neutron fluence. The sensitivity was obtained by using the output of the

sensor subtracted the zero-level drift. A non-linearity was observed as in pre-irradiation tests. In this figure, deviation of sensitivity from the fitting line is less than 6 %. After the operation of the reactor starts, the change of the sensitivity was small up to the fluence of about $8.1 \times 10^{20} \text{ n/m}^2$ as shown in Fig.10 (a). In this phase, the temperature near the strain gauge, which was measured by the thermocouple, was gradually increased. At full power, its temperature was kept constant, but its value was 110~117 °C because the temperature could not be raised to 200 °C due to a trouble of the temperature regulation system of JMTR capsule. In the full power region, the sensitivity indicates a gradual decrease with fluence up to the fluence of about $2.8 \times 10^{23} \text{ n/m}^2$ as shown in Fig.10 (b). The sensitivity was decreased by about 30 % at maximum from that before irradiation at the neutron fluence of $(1.8 \sim 2.8) \times 10^{23} \text{ n/m}^2$ in the high magnetic field. Beyond this fluence, the sensitivity was increased gradually in the high magnetic field or kept constant in the low magnetic field. Resistances of strain gauges were increased up to the fluence of about $7.3 \times 10^{22} \text{ n/m}^2$ after keeping constant temperature (110~117 °C) in the full power operation of JMTR. After that, resistances were decreased with the neutron fluence as shown in Fig.11. In this figure, an initial increase of resistances is due to temperature rise by the increase of the reactor power up to the fluence of about $9.5 \times 10^{21} \text{ n/m}^2$. The resistances of strain gauges are included the resistance of lead wires (MI-cables). The resistance of Al_2O_3 insulator between strain gauges and sensor beam (SS316L) was kept more than 10 MΩ during irradiation. The behaviour of the sensitivity is not fully understood, but the decrease of the sensitivity may be due to the change of resistance of strain gauges and/or the increase of the Young's modulus of the stainless steel that is used in the sensor beam by some effect of the neutron irradiation. The irradiation test has been completed on March 23 in 2001. The fluence is $\sim 1 \times 10^{24} \text{ n/m}^2$. The results will be reported in the task of T492 irradiation phase II.

6. Summary

The improved magnetic $\mathbf{j} \times \mathbf{B}$ sensor has been designed. The basic structure of the sensor is similar to the previously developed sensor (old sensor) in EDA phase. Materials of the load cell, which consists of the strain gauges, sensor beam and sensing coil/frame are selected considering the neutron resistance. A mineral insulated cable (MI-cable) is used as a cable of the sensing coil and solenoid coils. In

order to reduce the temperature drift of the sensor output, 4 strain gauges with the same electrical property and the same geometrical size are bonded on the sensor beam in a bridge arrangement by using Al_2O_3 plasma spraying process.

The zero-level drift, linearity and sensitivity of the output of the magnetic $\mathbf{j} \times \mathbf{B}$ sensor were investigated in the heating ($\text{RT} \sim 200^\circ\text{C}$), weight ($0 \sim 20 \text{ g}$) and magnetic field ($0 \sim 250 \text{ Gauss}$) tests. The drift of the output of the load cell was reduced to about $1/20$ of the old sensor. The temperature dependence of the output of the load cell is small. A non-linearity was observed against weight and magnetic field in pre-irradiation and irradiation tests. The sensitivity was decreased by $\sim 30\%$ compared with that in pre-irradiation at neutron fluence of $(1.8 \sim 2.8) \times 10^{23} \text{ n/m}^2$ in the high magnetic field.

It is necessary to make a further improvement for the prototype sensor. The magnetic $\mathbf{j} \times \mathbf{B}$ sensor may be used in the radiation environment of ITER-FEAT although its sensitivity is decreased by the neutron irradiation. In actual application, it may be necessary to execute an in-situ calibration of the sensitivity by using the externally applied magnetic field.

Acknowledgements

The authors are grateful to Drs. T. Sugie, T. Nishitani, H. Kawamura (Oarai Research Establishment, JAERI), K. Yamaura (Oarai Research Establishment, JAERI) and K. Moriyama (Hitachi, Ltd) for their useful discussion. This paper has been prepared as an account of work assigned to the Japanese Home Team under Task agreement number N 55 TT 08 FJ within the Agreement among the European Atomic Energy Community, the Government of Japan, the Government of the Russian Federation and the Government of the United States of America on Cooperation in the Engineering Design Activities for the International Thermonuclear Experimental Reactor ("ITER EDA Agreement") under the auspices of the International Atomic Energy Agency (IAEA).

References

- [1] S. Hara, M. Abe and K. Moriyama : Development of a Magnetic Sensor for Nuclear Fusion Reactor, Proceedings of 12th autumn meeting held at Iwate

university in Japan, The Japan Society of Plasma Science and Nuclear Fusion Research, 1995, p85 (in Japanese).

- [2] S. Hara, M. Abe and K. Moriyama : Kakuyugo Kenkyu **73** (1997) 501-509.
- [3] Robert D. Woolley : Tokamak Poloidal Magnetic Field Measurements Accurate for Unlimited Time Duration, 16th IEEE/NPSS Symposium on Fusion Engineering, 1995, vol.2, p1530.
- [4] K. Matsuura, M. Sakata, S. Fujiwaka and J. Fujita : Kakuyugo Kenkyu **70** (1994) 397.
- [5] S. Hara, S. Kasai, T. Nishitani, A. Nagashima, and T. Nakayama : Rev. Sci. Instrum. **70** (1999) 435-438.
- [6] S. Hara, A. Nagashima, T. Nakayama, S. Kasai : JAERI-Tech 98-057 (December 1998).

This is a blank page.

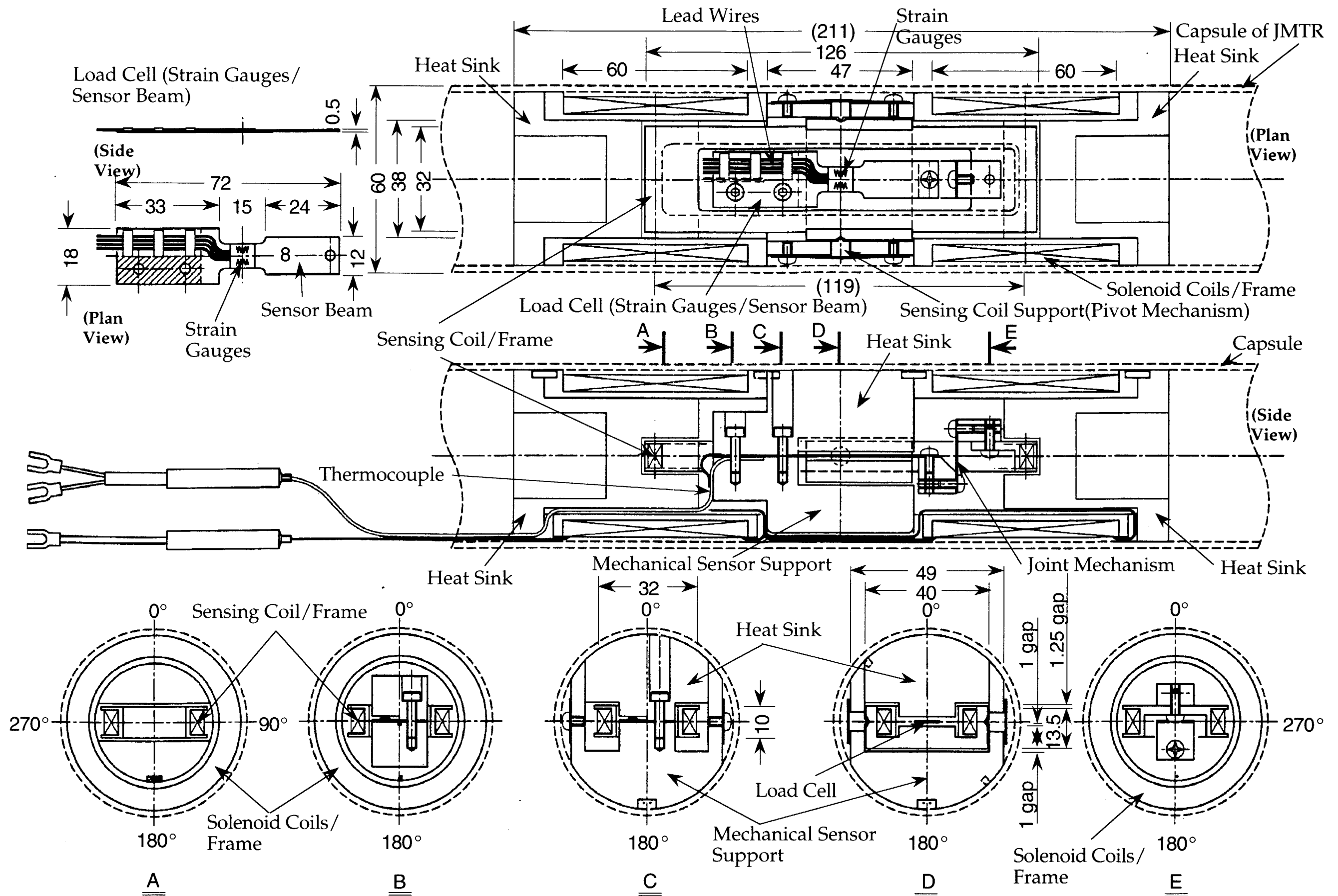


Fig.1 Plan and side views and cross-section of the designed magnetic $j \times B$ sensor (mechanical sensor).

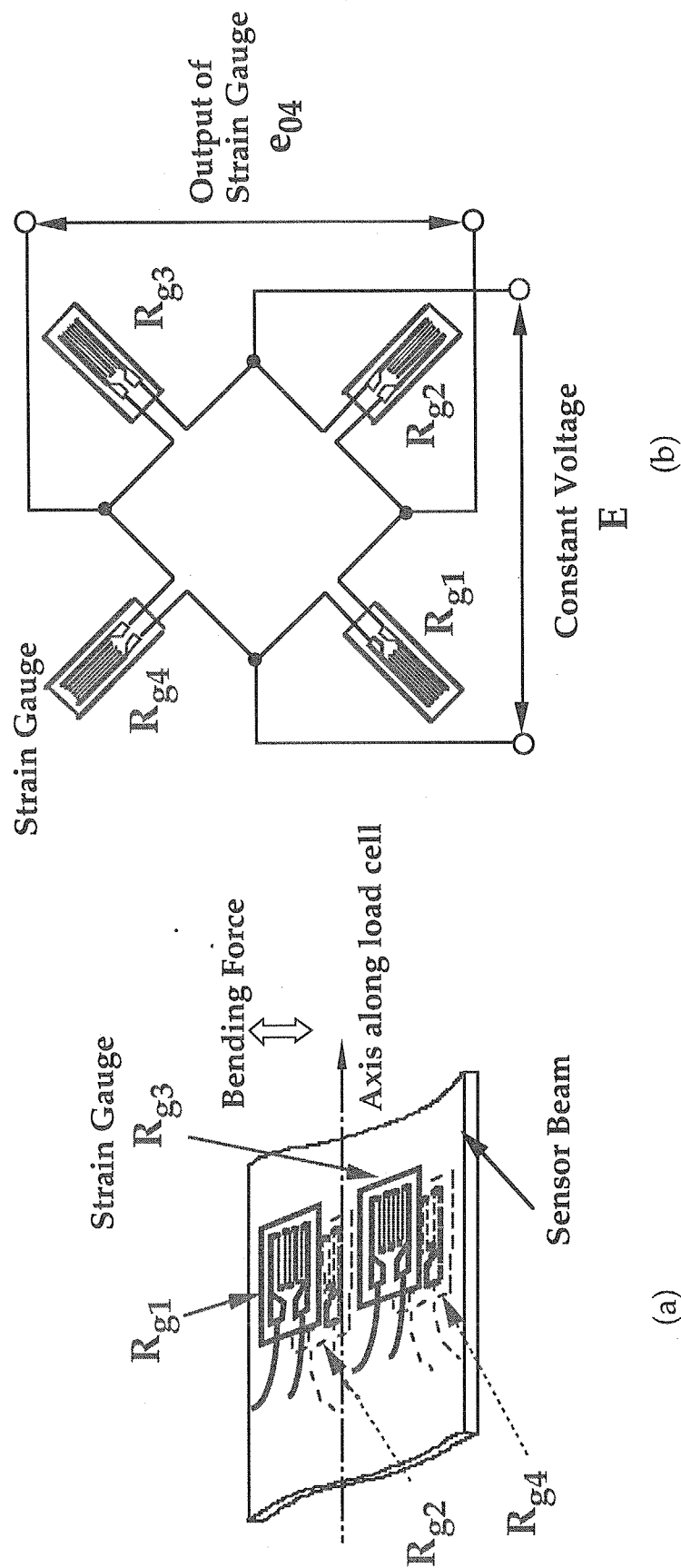


Fig.2 Strain gauges bonded on the sensor beam (a), Electrical bridge circuit formed by four strain gauges (b).

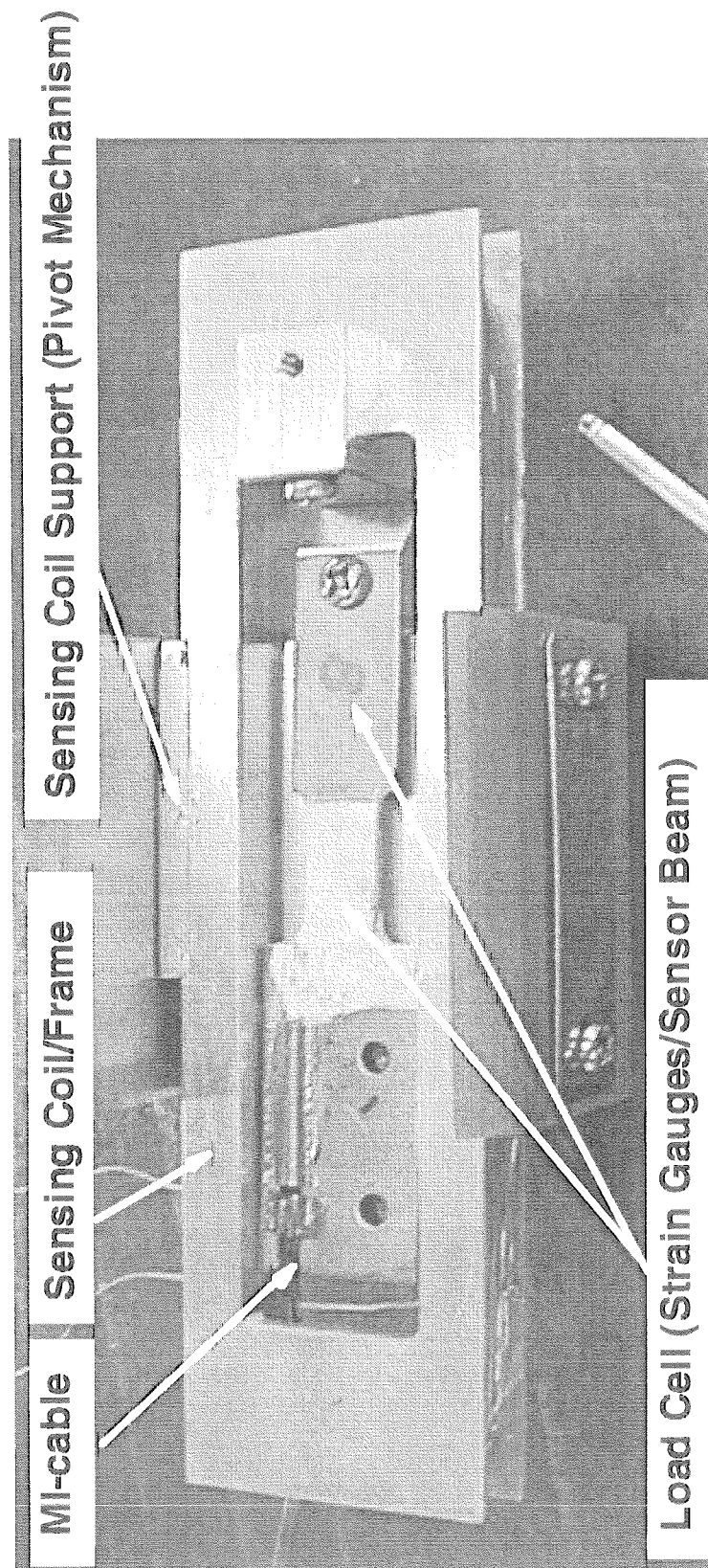


Fig.3 Photograph of the magnetic $j \times B$ sensor under assembling.

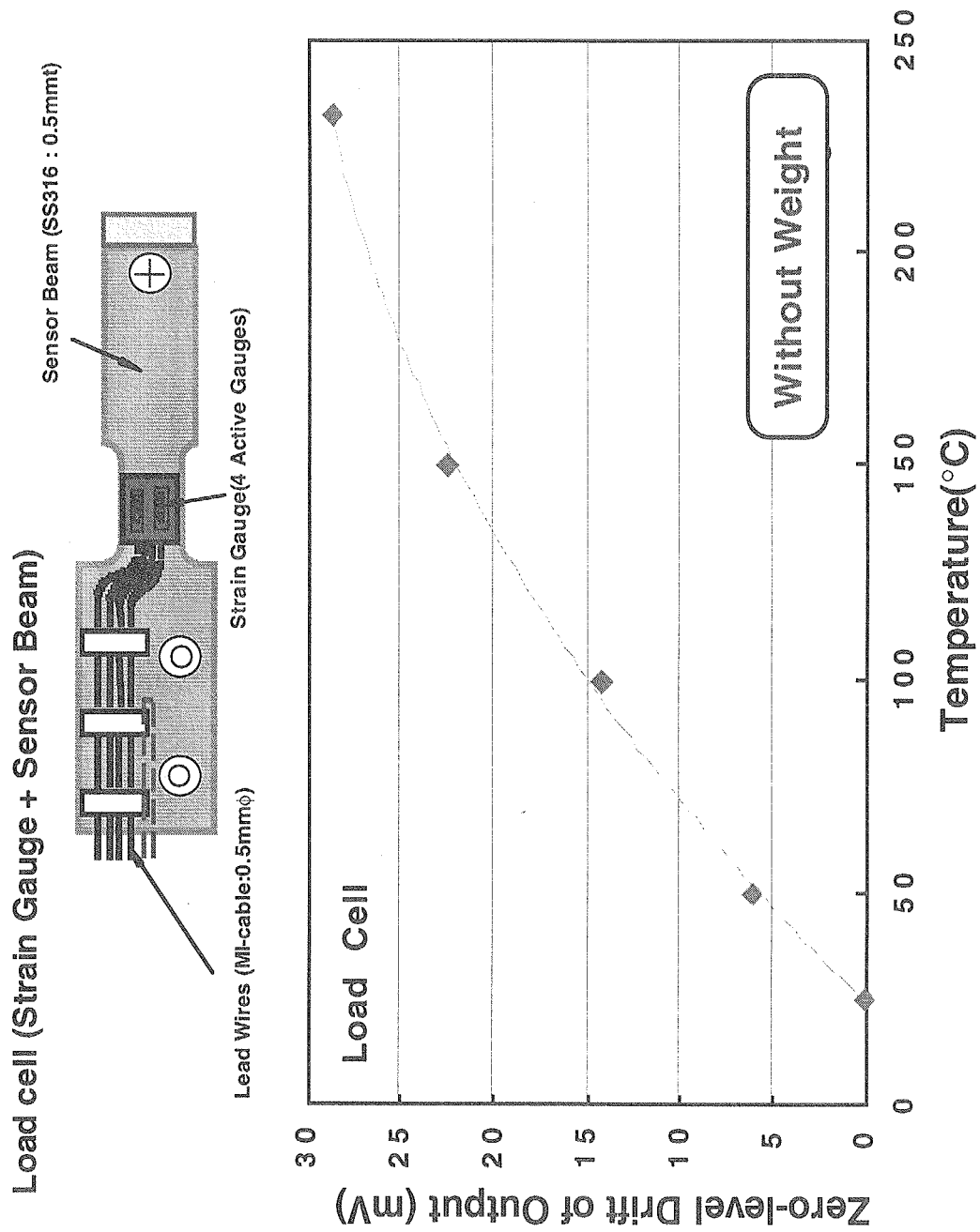


Fig.4 Dependence of the zero-level drift of the load cell on temperature.

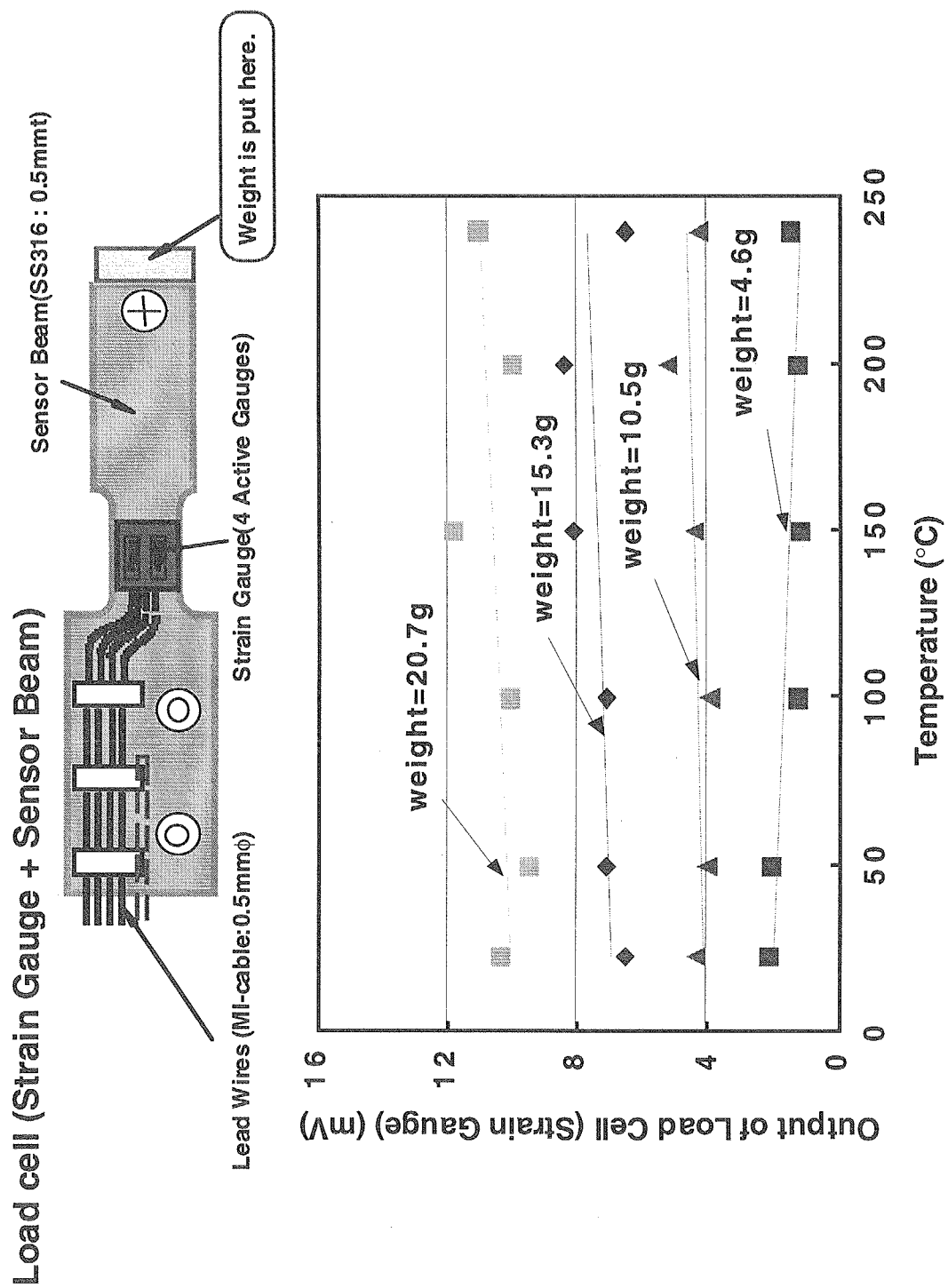


Fig.5 Dependence of the output of the load cell used in magnetic γ B sensor on temperature in different weights.

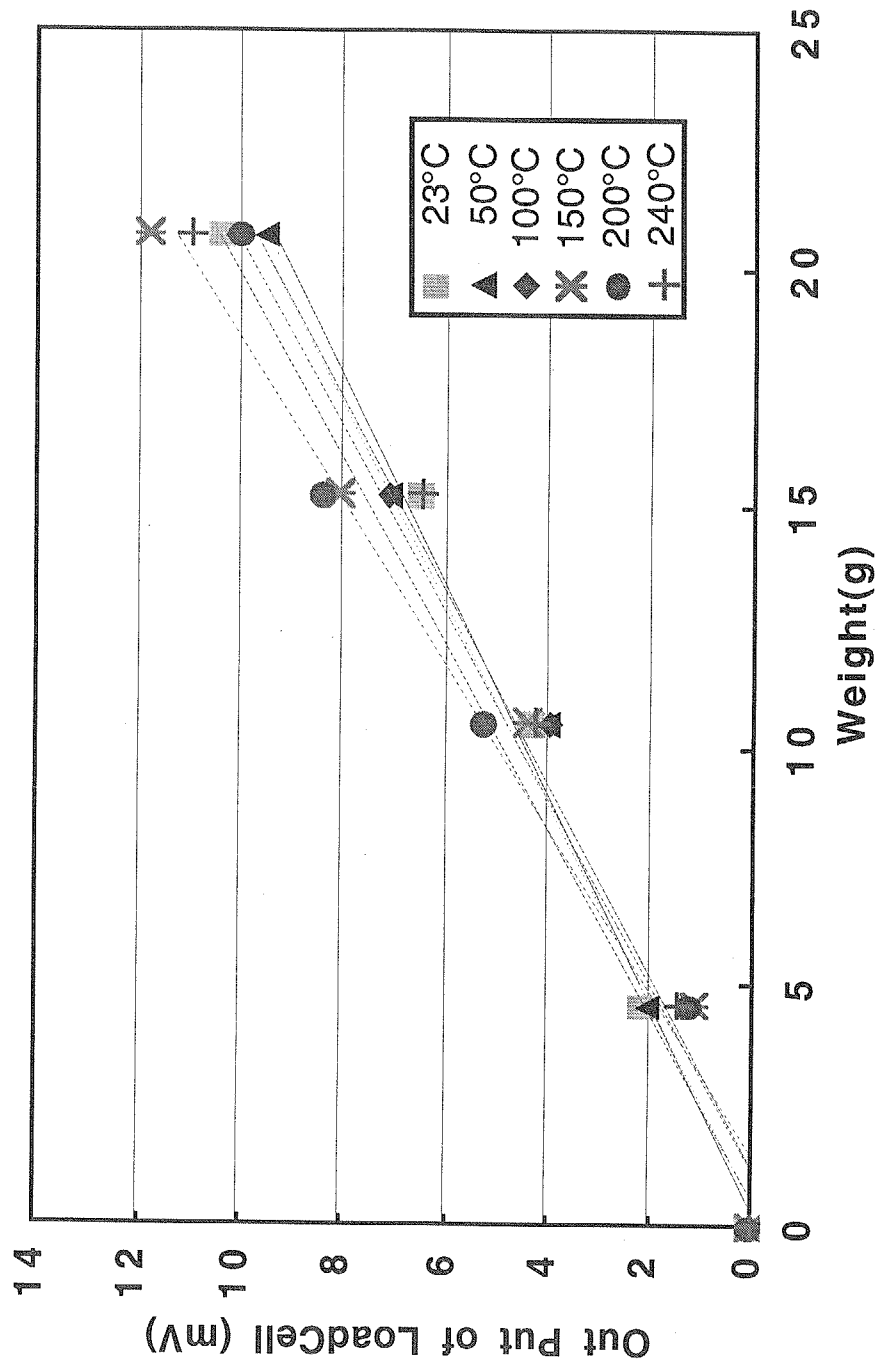


Fig.6 Dependence of the output of the load cell used in magnetic jxB sensor on weight in different temperatures.

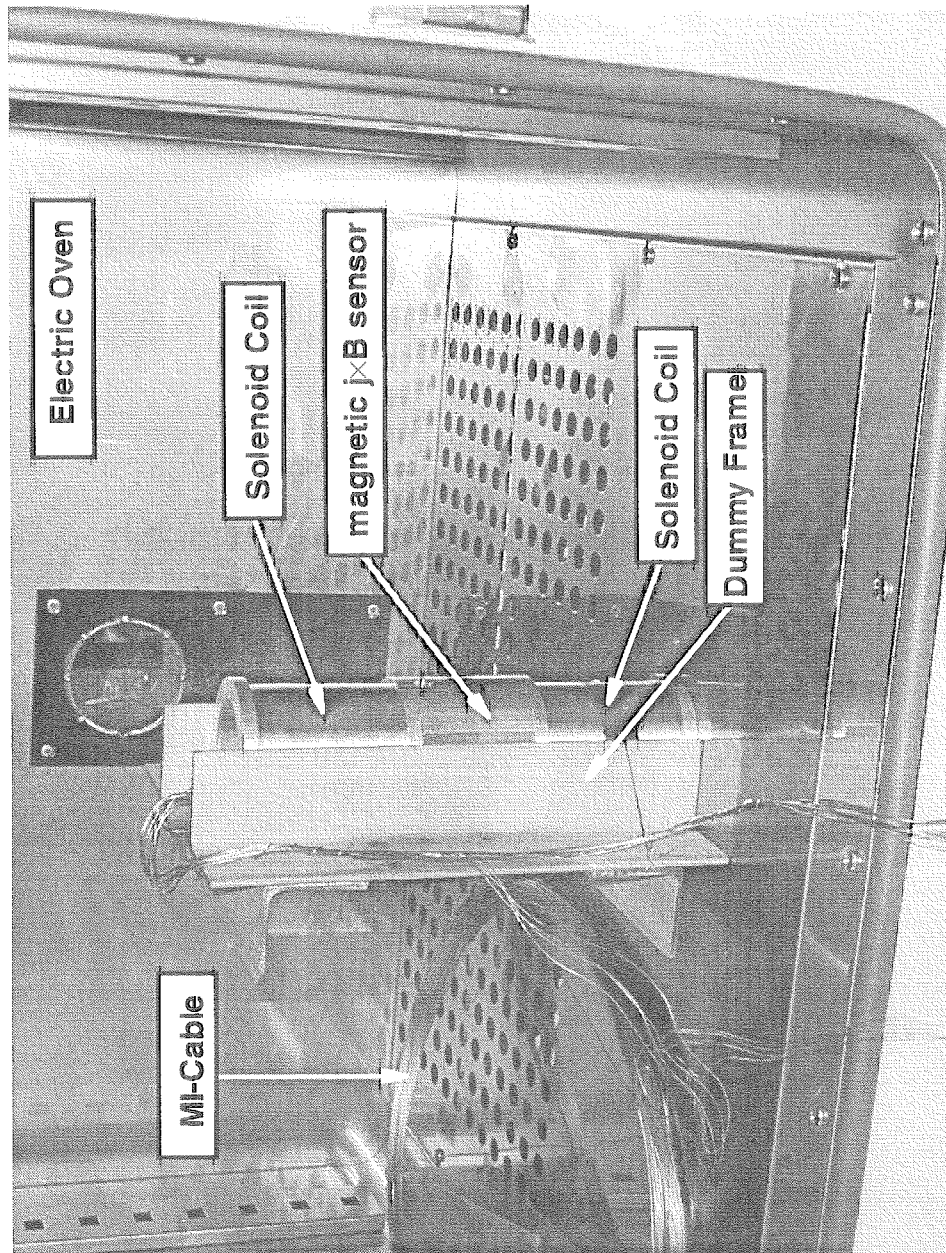


Fig.7 Photograph of heating test of magnetic $\times B$ sensor using an electric oven.

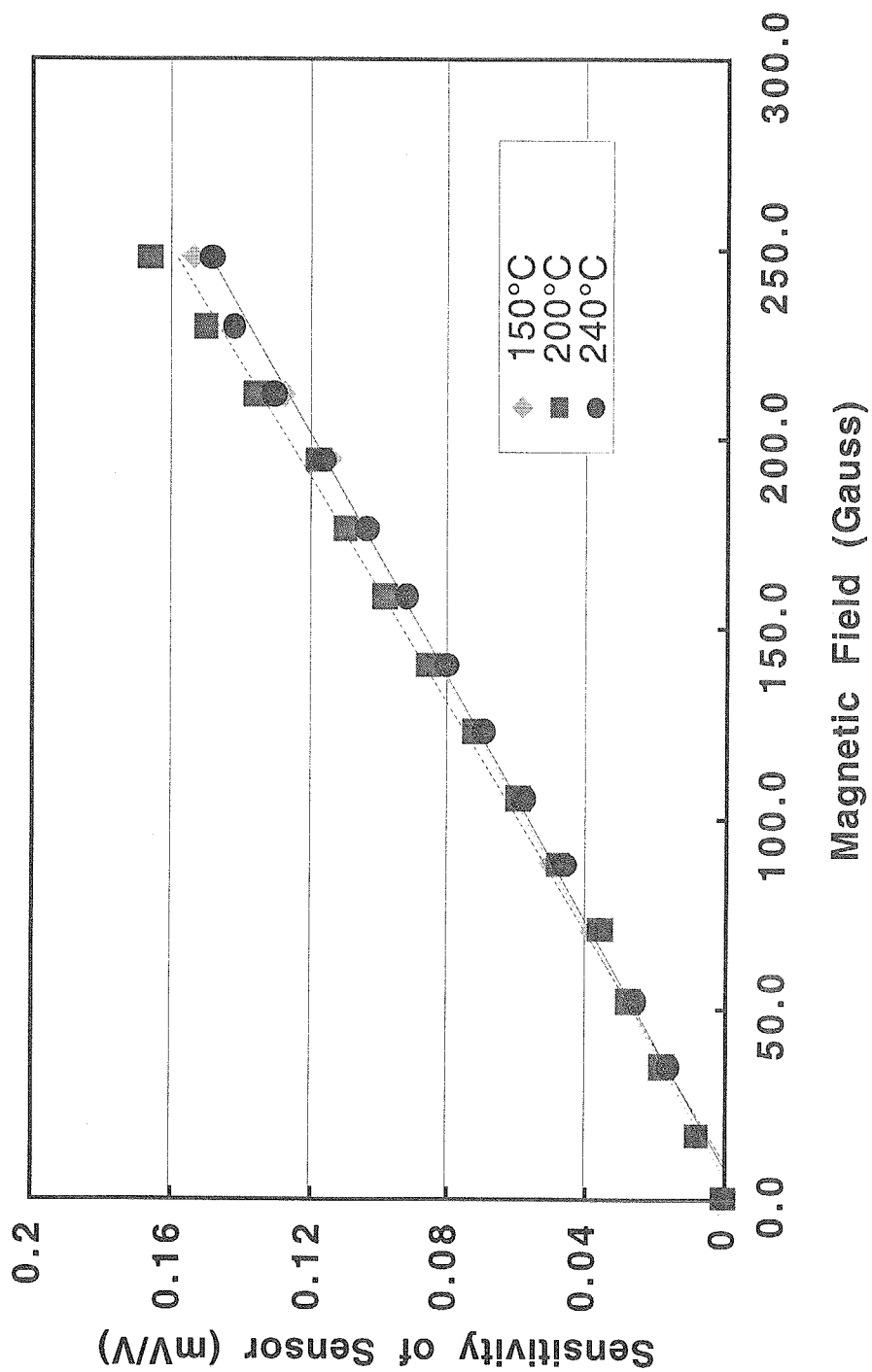


Fig.8 Sensitivity of the magnetic $j \times B$ sensor versus magnetic field at temperature of 150, 200 and 240°C, which are the temperature near the strain gauges monitored by thermocouple.

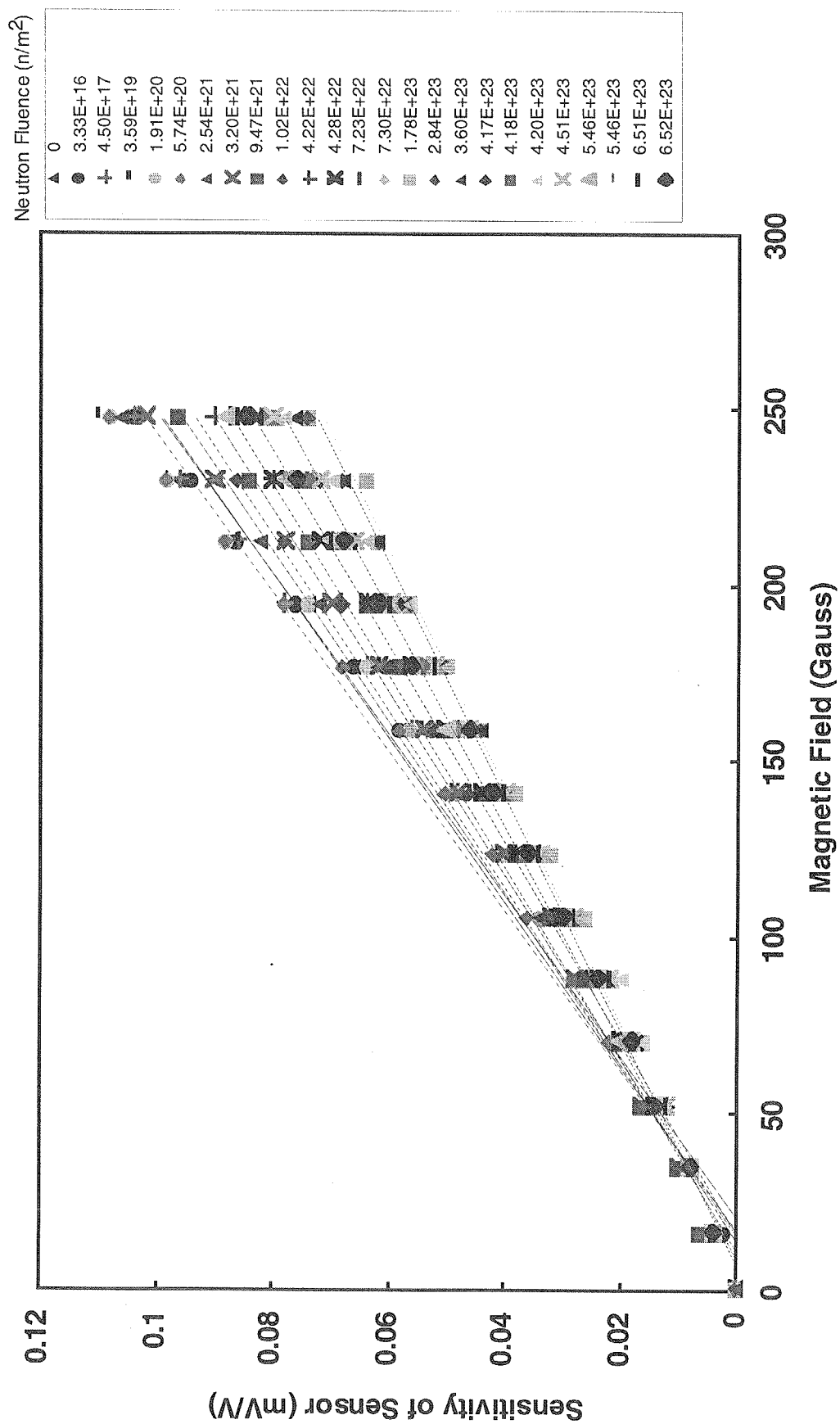


Fig. 9 Sensitivity of the magnetic $j \times B$ sensor versus magnetic field in difference neutron fluences.

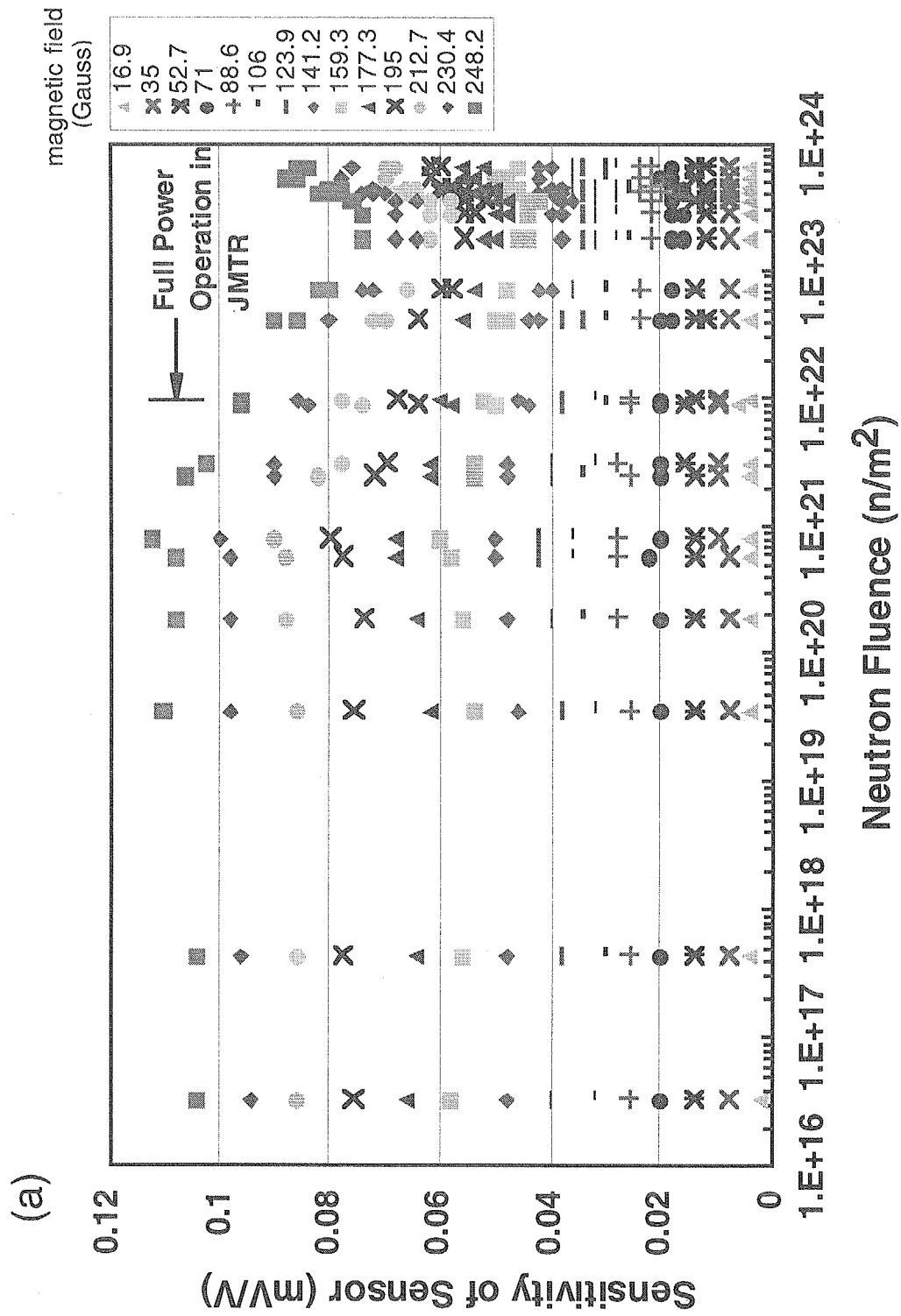


Fig. 10 (a) Sensitivity of magnetic $j \times B$ sensor versus neutron fluence in difference magnetic field. The horizontal axis is logarithmic scale.

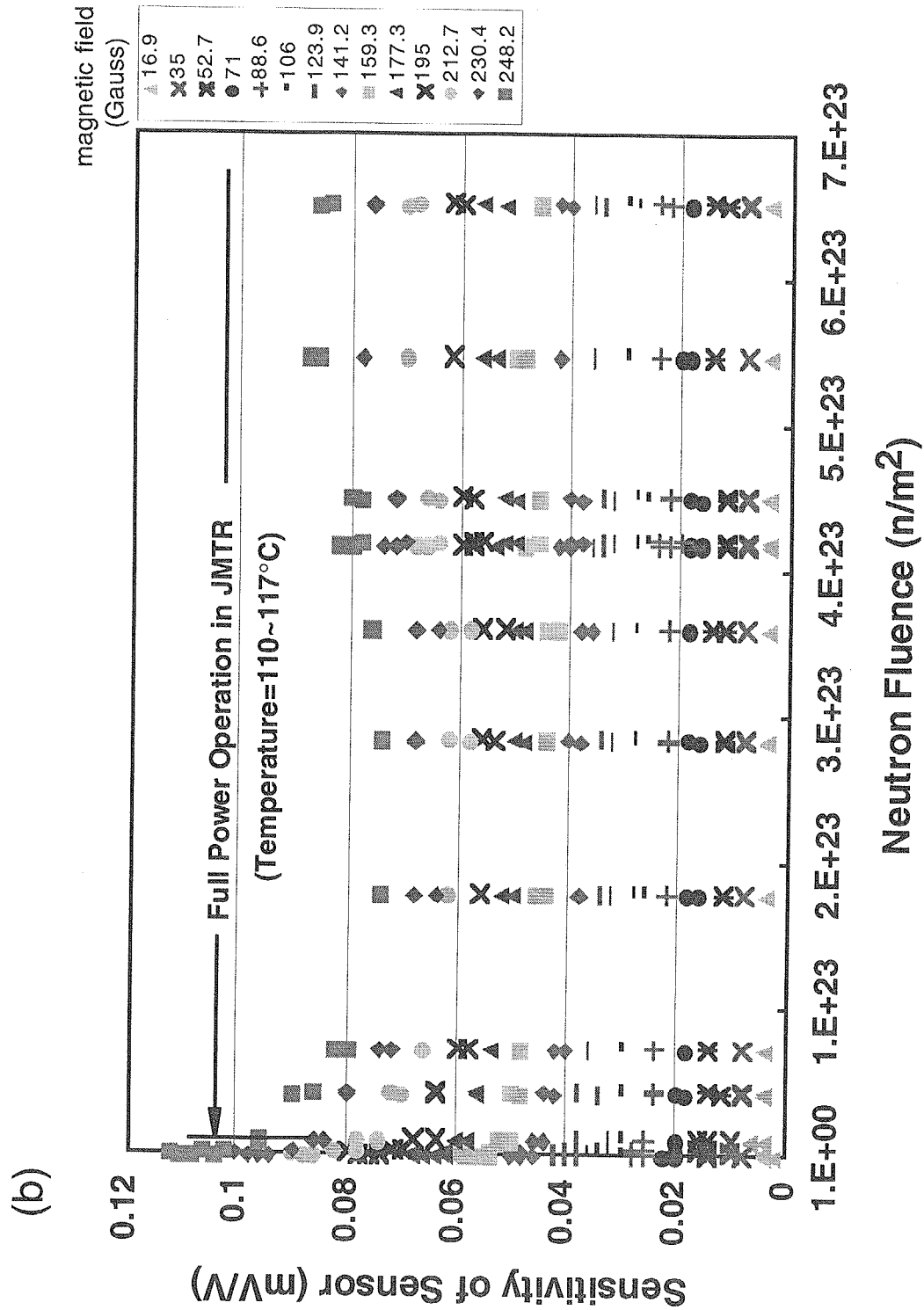


Fig. 10 (b) Sensitivity of magnetic jxB sensor versus neutron fluence in difference magnetic field. The horizontal axis is linear scale and the expanded graph in full power region in Fig.10 (a).

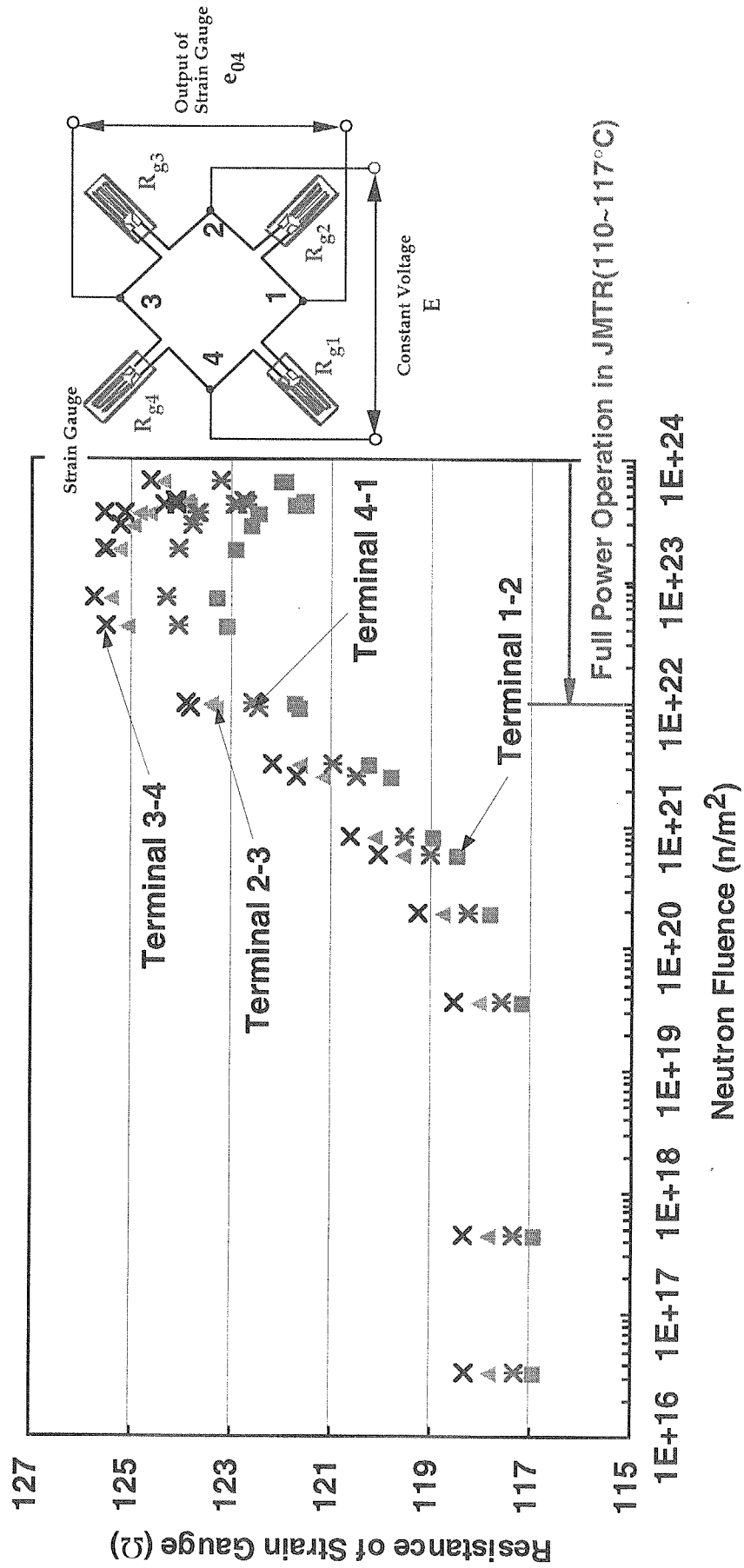


Fig. 11 Resistance of strain gauges between each terminal versus neutron fluence.

This is a blank page.

国際単位系 (SI) と換算表

表1 SI基本単位および補助単位

量	名 称	記 号
長 さ	メ ー ト ル	m
質 量	キ ロ グ ラ ム	kg
時 間	秒	s
電 流	ア ン ペ ア	A
熱力学温度	ケ ル ビ ン	K
物 質 量	モ ー ル	mol
光 度	カ ン デ ラ	cd
平 面 角	ラ ジ ア ン	rad
立 体 角	ステラジアン	sr

表3 固有の名称をもつSI組立単位

量	名 称	記号	他のSI単位 による表現
周 波 数	ヘ ル ツ	Hz	s ⁻¹
力	ニ ュ ー ト ン	N	m·kg/s ²
圧 力, 応 力	パ ス カ ル	Pa	N/m ²
エネルギー, 仕事, 熱量	ジ ュ ー ル	J	N·m
工 率, 放 射 束	ワ ッ ト	W	J/s
電 気 量, 電 荷	ク ー ロ ン	C	A·s
電位, 電圧, 起電力	ボ ル ト	V	W/A
静 電 容 量	フ ァ ラ ド	F	C/V
電 気 抵 抗	オ ー ム	Ω	V/A
コンダクタンス	ジ ー メ ン ス	S	A/V
磁 束	ウ ェ ー バ	Wb	V·s
磁 束 密 度	テ ス ラ	T	Wb/m ²
インダクタンス	ヘ ン リ ー	H	Wb/A
セルシウス温度	セルシウス度	°C	
光 束	ル ー メ ン	lm	cd·sr
照 度	ル ク ス	lx	lm/m ²
放 射 能	ベ ク レ ル	Bq	s ⁻¹
吸 収 線 量	グ レ イ	Gy	J/kg
線 量 当 量	シーベル	Sv	J/kg

表2 SIと併用される単位

名 称	記 号
分, 時, 日	min, h, d
度, 分, 秒	°, ', "
リットル	l, L
トン	t
電子ボルト	eV
原子質量単位	u

$$1 \text{ eV} = 1.60218 \times 10^{-19} \text{ J}$$

$$1 \text{ u} = 1.66054 \times 10^{-27} \text{ kg}$$

表4 SIと共に暫定的に維持される単位

名 称	記 号
オングストローム	Å
バ ー ン	b
バ ー ル	bar
ガ ル	Gal
キ ュ リ ー	Ci
レ ン ト ゲ ン	R
ラ ド	rad
レ ム	rem

$$1 \text{ Å} = 0.1 \text{ nm} = 10^{-10} \text{ m}$$

$$1 \text{ b} = 100 \text{ fm} = 10^{-28} \text{ m}^2$$

$$1 \text{ bar} = 0.1 \text{ MPa} = 10^5 \text{ Pa}$$

$$1 \text{ Gal} = 1 \text{ cm/s}^2 = 10^{-2} \text{ m/s}^2$$

$$1 \text{ Ci} = 3.7 \times 10^{10} \text{ Bq}$$

$$1 \text{ R} = 2.58 \times 10^{-4} \text{ C/kg}$$

$$1 \text{ rad} = 1 \text{ cGy} = 10^{-2} \text{ Gy}$$

$$1 \text{ rem} = 1 \text{ cSv} = 10^{-2} \text{ Sv}$$

表5 SI接頭語

倍数	接頭語	記 号
10 ¹⁸	エクサ	E
10 ¹⁵	ペタ	P
10 ¹²	テラ	T
10 ⁹	ギガ	G
10 ⁶	メガ	M
10 ³	キロ	k
10 ²	ヘクト	h
10 ¹	デカ	da
10 ⁻¹	デシ	d
10 ⁻²	センチ	c
10 ⁻³	ミリ	m
10 ⁻⁶	マイクロ	μ
10 ⁻⁹	ナノ	n
10 ⁻¹²	ピコ	p
10 ⁻¹⁵	フェムト	f
10 ⁻¹⁸	アト	a

(注)

- 表1・5は「国際単位系」第5版, 国際度量衡局 1985年刊行による。ただし, 1 eV および 1 u の値は CODATA の 1986 年推奨値によった。
- 表4には海里, ノット, アール, ヘクトールも含まれているが日常の単位なのでここでは省略した。
- bar は, JIS では流体の圧力を表わす場合に限り表2のカテゴリーに分類されている。
- EC 閣僚理事会指令では bar, barn および「血圧の単位」mmHg を表2のカテゴリーに入れている。

換 算 表

力	N (=10 ⁵ dyn)	kgf	lbf
	1	0.101972	0.224809
	9.80665	1	2.20462
	4.44822	0.453592	1

$$\text{粘 度 } 1 \text{ Pa} \cdot \text{s} (\text{N} \cdot \text{s} / \text{m}^2) = 10 \text{ P (ポアズ)} (\text{g} / (\text{cm} \cdot \text{s}))$$

$$\text{動粘度 } 1 \text{ m}^2 / \text{s} = 10^4 \text{ St (ストークス)} (\text{cm}^2 / \text{s})$$

圧	MPa (=10 bar)	kgf/cm ²	atm	mmHg (Torr)	lbf/in ² (psi)
	1	10.1972	9.86923	7.50062 × 10 ³	145.038
力	0.0980665	1	0.967841	735.559	14.2233
	0.101325	1.03323	1	760	14.6959
	1.33322 × 10 ⁻⁴	1.35951 × 10 ⁻³	1.31579 × 10 ⁻³	1	1.93368 × 10 ⁻²
	6.89476 × 10 ⁻³	7.03070 × 10 ⁻²	6.80460 × 10 ⁻²	51.7149	1

エネルギー・仕事・熱量	J (=10 ⁷ erg)	kgf·m	kW·h	cal (計量法)	Btu	ft·lbf	eV
	1	0.101972	2.77778 × 10 ⁻⁷	0.238889	9.47813 × 10 ⁻⁴	0.737562	6.24150 × 10 ¹⁸
	9.80665	1	2.72407 × 10 ⁻⁶	2.34270	9.29487 × 10 ⁻³	7.23301	6.12082 × 10 ¹⁹
	3.6 × 10 ⁶	3.67098 × 10 ⁵	1	8.59999 × 10 ⁵	3412.13	2.65522 × 10 ⁶	2.24694 × 10 ²⁵
	4.18605	0.426858	1.16279 × 10 ⁻⁶	1	3.96759 × 10 ⁻¹	3.08747	2.61272 × 10 ¹⁹
	1055.06	107.586	2.93072 × 10 ⁻⁴	252.042	1	778.172	6.58515 × 10 ²¹
	1.35582	0.138255	3.76616 × 10 ⁻⁷	0.323890	1.28506 × 10 ⁻³	1	8.46233 × 10 ¹⁸
	1.60218 × 10 ⁻¹⁹	1.63377 × 10 ⁻²⁰	4.45050 × 10 ⁻²⁶	3.82743 × 10 ⁻²⁰	1.51857 × 10 ⁻²²	1.18171 × 10 ⁻¹⁹	1

$$1 \text{ cal} = 4.18605 \text{ J (計量法)}$$

$$= 4.184 \text{ J (熱化学)}$$

$$= 4.1855 \text{ J (15 °C)}$$

$$= 4.1868 \text{ J (国際蒸気表)}$$

$$\text{仕事率 } 1 \text{ PS (仏馬力)}$$

$$= 75 \text{ kgf} \cdot \text{m/s}$$

$$= 735.499 \text{ W}$$

放射能	Bq	Ci
	1	2.70270 × 10 ⁻¹¹
	3.7 × 10 ¹⁰	1

吸収線量	Gy	rad
	1	100
	0.01	1

照射線量	C/kg	R
	1	3876
	2.58 × 10 ⁻⁴	1

線量当量	Sv	rem
	1	100
	0.01	1

(86年12月26日現在)

